

Investigating the Ceboruco Volcano (Mexico) using the complex MT Apparent Resistivity Tensor

P. Hering¹, A. Junge¹, C. Brown², L. Gonzalez-Castillo³

1. Institute of Geosciences, Goethe University Frankfurt am Main; 2. Ryan Institute, National University of Ireland, Galway, Ireland; 3. Dpto. de Geodinámica, Universidad de Granada, Granada, Spain

Introduction

The Ceboruco is a 2280 m high stratovolcano located in Nayarit State, Mexico. Despite its last eruption which occurred in 1870, it is the most active volcano in the area, showing volcanic-earthquake activity together with ongoing vapor emissions. The magnetotelluric survey was carried out in November 2016. It was part of a geothermal project (*CeMIEGeo-P24*) and focused on the determination of the electrical conductivity distribution in the subsurface of the volcano.

The Magnetotelluric Apparent Resistivity Tensor, as introduced by *Brown (2016)*, can be decomposed into an amplitude and a phase tensor. The fundamental physics behind those new tensors were presented in *Hering et al. (2019)*, using canonical models in 1-D (isotropic and anisotropic) and 2-D resistivity environments. Here, the tensors are introduced for a high-quality data set, where their interpretational benefits become very obvious. Additionally, results from an isotropic 3-D inversion are presented and compared to an alternative 3-D anisotropic forward model.

The CART

The complex Magnetotelluric (MT) Apparent Resistivity Tensor (CART) was introduced by *Brown (2016)*:

$$\rho_a = (i\mu/\omega) \det(\mathbf{Z}) \mathbf{Z} \mathbf{Y}^T$$

with \mathbf{Z} being the Impedance Tensor, \mathbf{Y} the inverse Impedance Tensor, ω the angular frequency and μ the magnetic permeability. It can be decomposed into two real tensors, the Apparent Resistivity and the Apparent Resistivity Phase Tensors (*Hering et al., 2019*):

$$\rho_a = U_a + iV_a = U_a(I + iU_a^{-1}V_a) = U_a(I + i\phi_a)$$

giving U_a and ϕ_a as the Resistivity (RT) and the Resistivity Phase Tensor (RPT), respectively. They represent relationships between the observed electric field at a point on the Earth's surface and the associated apparent current density. In **Figure 1** the frequency dependent tensor responses are compared for an anisotropic 1-D model (2 km thick anisotropic layer at 2 km depth; ρ_x : 10 Ωm , ρ_y : 1000 Ωm).

The Measurement Area

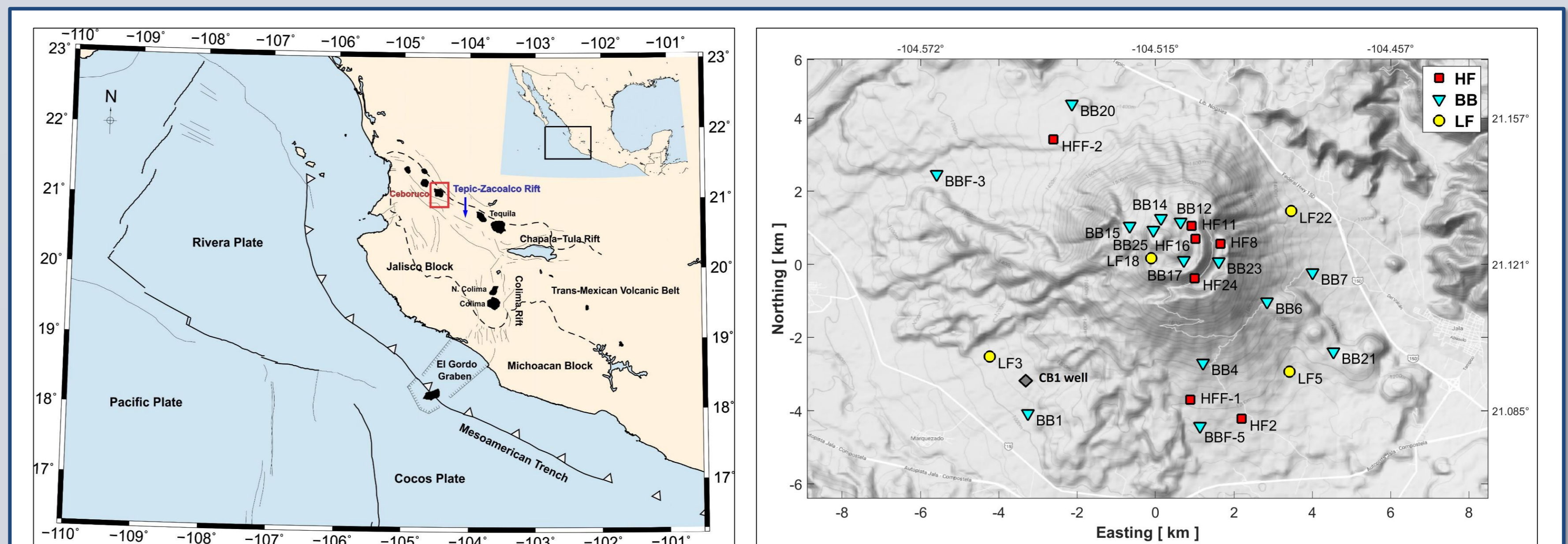


Fig. 2: The Ceboruco is placed in the central part of the Tepic-Zacoalco Rift (TZR), which constitutes the northwestern end of the Trans-Mexican Volcanic Belt. Together with Chapala and Colima (in the Jalisco Block), they form the triple rift system developed as consequence of the ongoing subduction of the Rivera and Cocos oceanic plates beneath the North American continental crust (see left picture). The right picture shows the station setup in the measurement area.

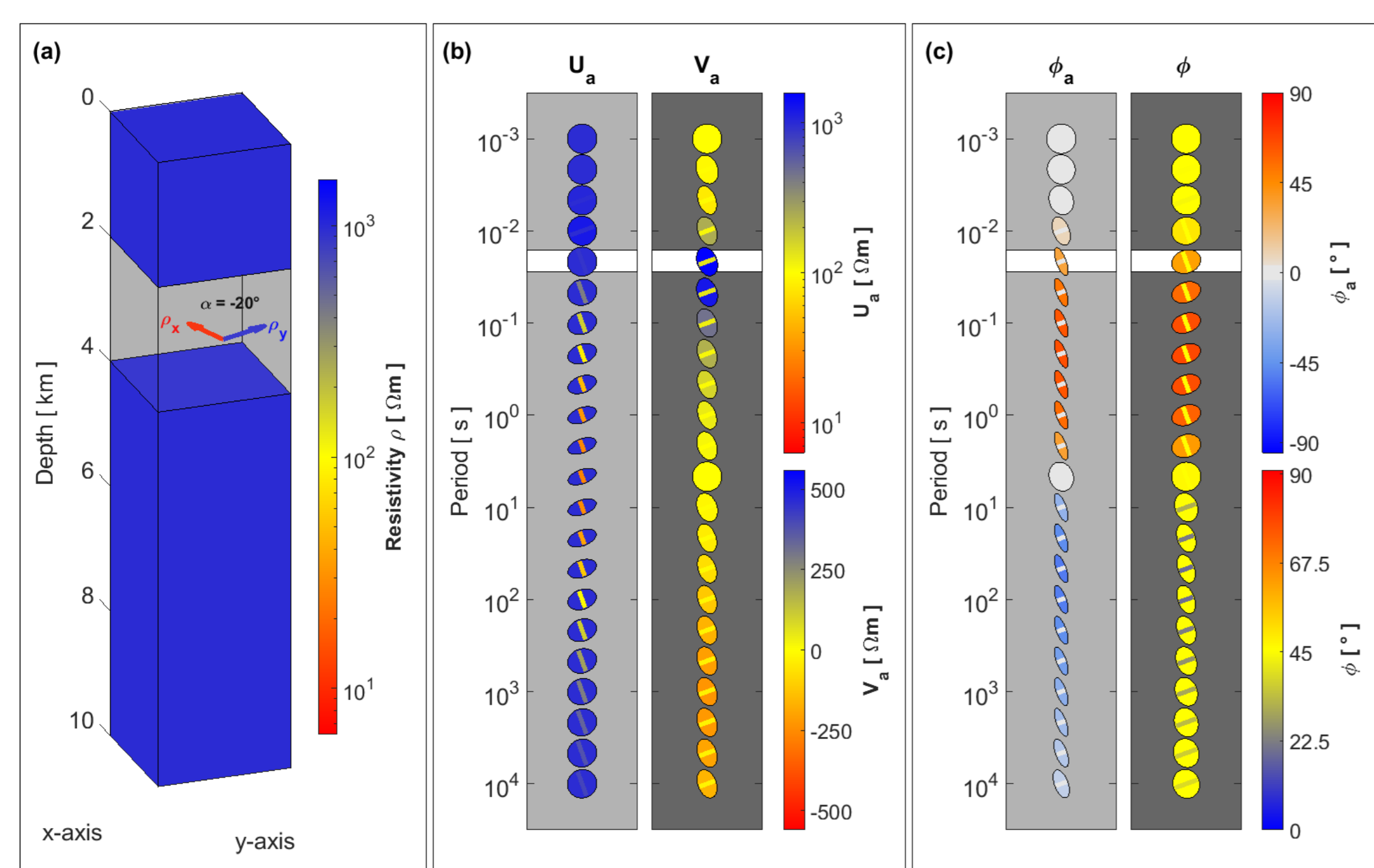


Fig. 1: Results from a 1-D anisotropic forward model. (a) The resistivity model. (b) Period dependence of the RT (U_a) and the imaginary part of the CART (V_a). For periods > 0.05 s, both tensors show the direction of the anisotropy. The RT exclusively presents apparent resistivity values. (c) RPT (ϕ_a) and conventional PT (ϕ) (Caldwell et al., 2004). For periods from 0.05 to 5 s (sensitive to the anisotropic body) the minor and major axes have opposite directions. (Figure from *Hering et al., 2019*)

Processing Results

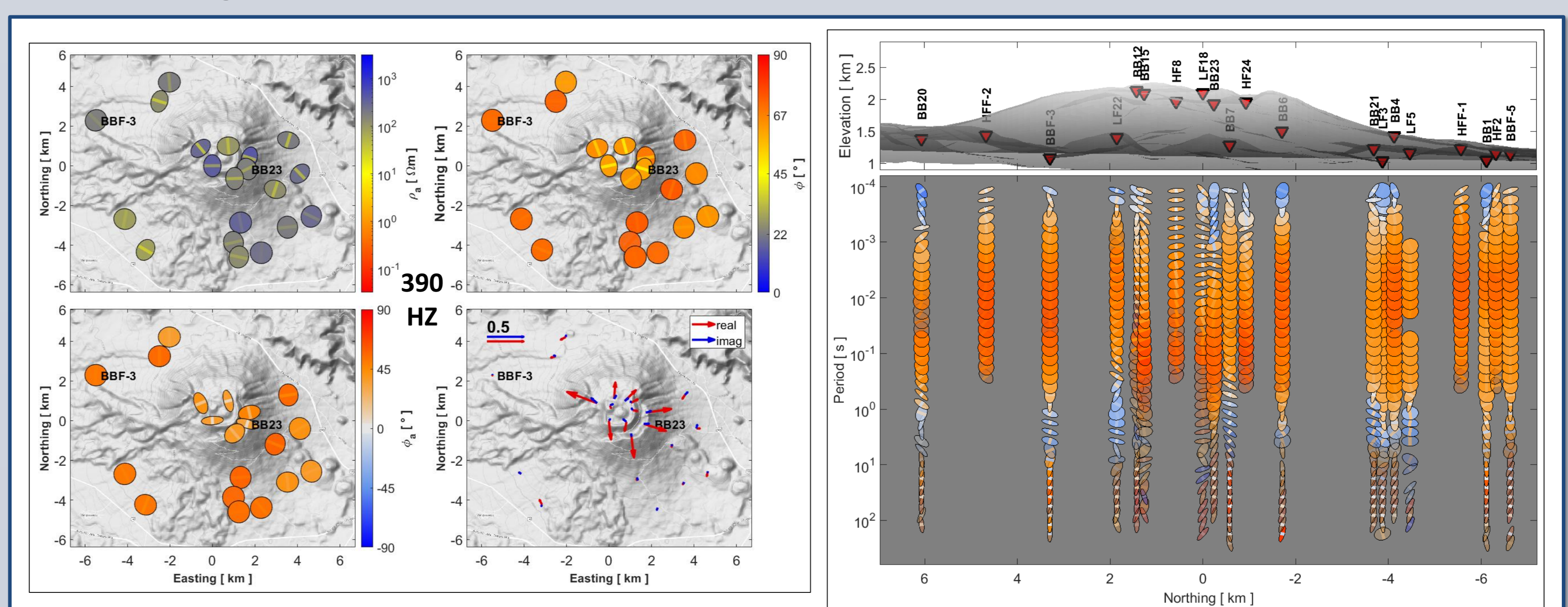


Fig. 3: Processing results for the Ceboruco volcano were obtained using a robust multivariate processing scheme (*Hering, 2019*, following *Egbert, 1997*). Left: RT (U_a), PT (ϕ), RPT (ϕ_a) and Induction vectors for a frequency of 390 Hz. Stations in the foreland show a 1-D pattern, whilst sites on the volcano feature strong topographic effects. Right: Frequency dependent RPT response projected on a N-S profile (color scale see left plot). The highest frequencies show distortion effects, either due to topography or near surface anomalies. Between ~ 1 kHz and 1 s high phase values indicate a transition to a conductor. For periods from 1 – 10 s, negative RPT major axes indicate a resistor; to the long-period end, a spatially consistent split in the tensor principal axes arises.

Isotropic 3-D Inversion Results

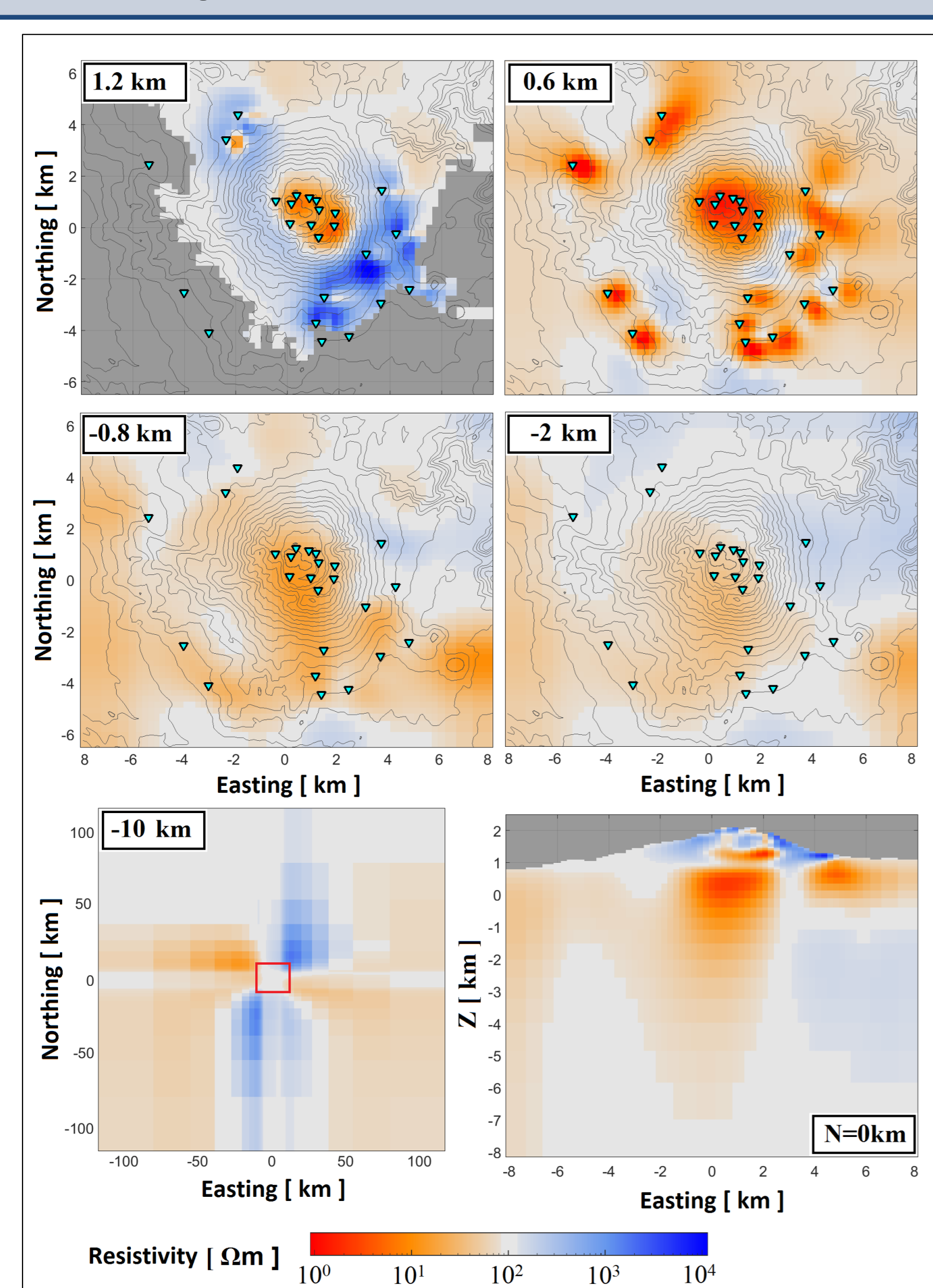


Fig. 4: 3-D Inversion results, visualized by 5 depth slices and one vertical cross-section. The results show a conductive feature within the volcanic edifice and a conductive layer between approx. 1 and -2 km. At 10 km depth, the inversion creates large resistivity contrasts reaching far outside the measurement area.

Data fit at 55 s

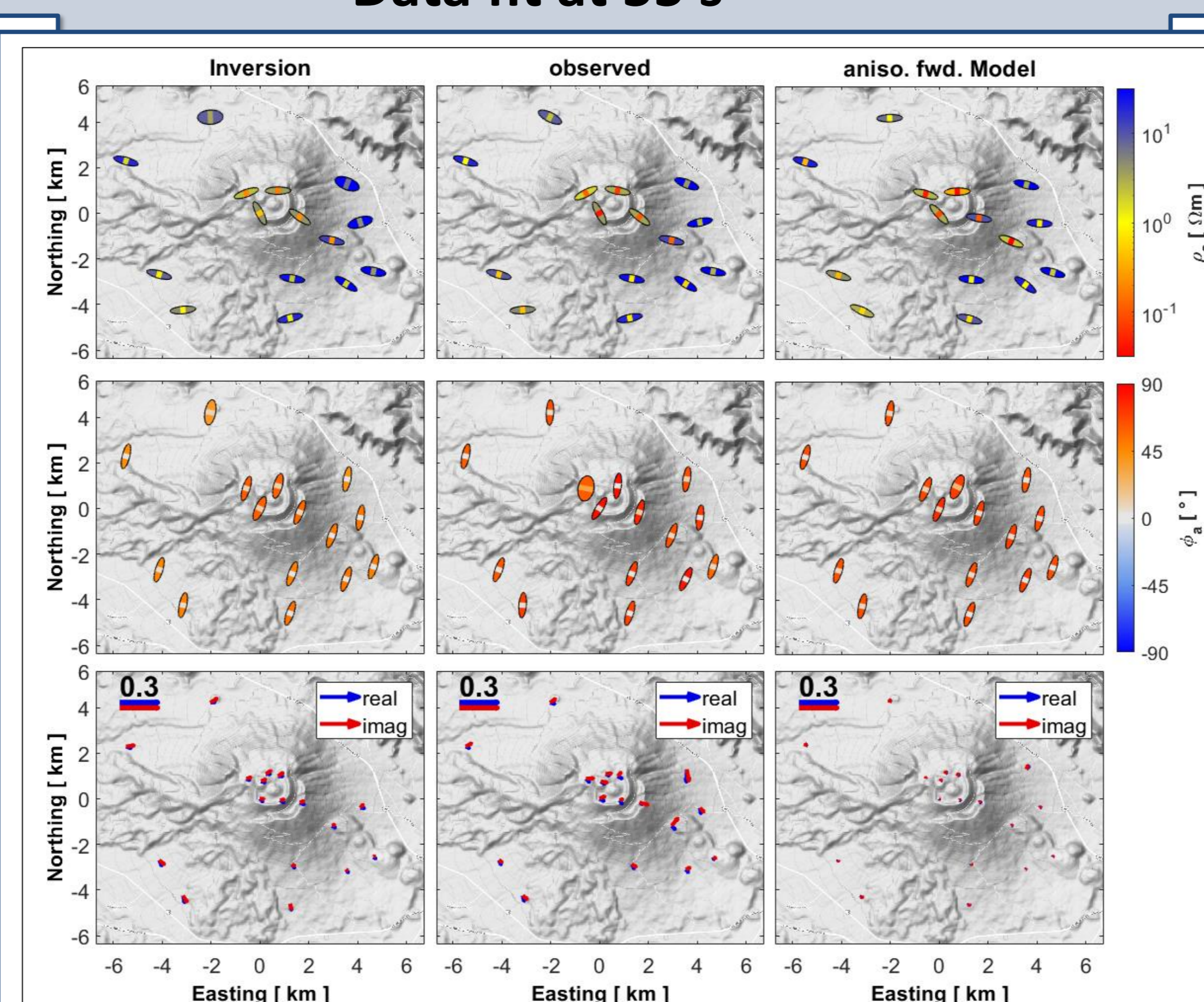


Fig. 6: Data fit for a target period of 55 s. Shown are the RT, RPT and Tipplers (top to bottom). The overall data fit (all frequencies) of the inversion is excellent (RMS 1.05) but for the long periods (shown here) there is a systematic misfit of the RPT major and the RT minor axes. This is improved by the anisotropic forward model.

Inversion setup: The inversion was performed using the ModEM inversion code (Kelbert et al., 2014). The starting model was 100 Ωm , the covariance smoothing 0.3 (x, y, z) and the horizontal and vertical cell size in the inner model 230 and 50 m, respectively. In the outer model, the cell size was increased by a factor of 1.2 till a maximum model size of 420 x 420 x 220 km^3 . The inversion was calculated for \mathbf{Z} and $\bar{\mathbf{T}}$ (16 periods, 10^3 – 200 s).

Anisotropic 3-D forward Model

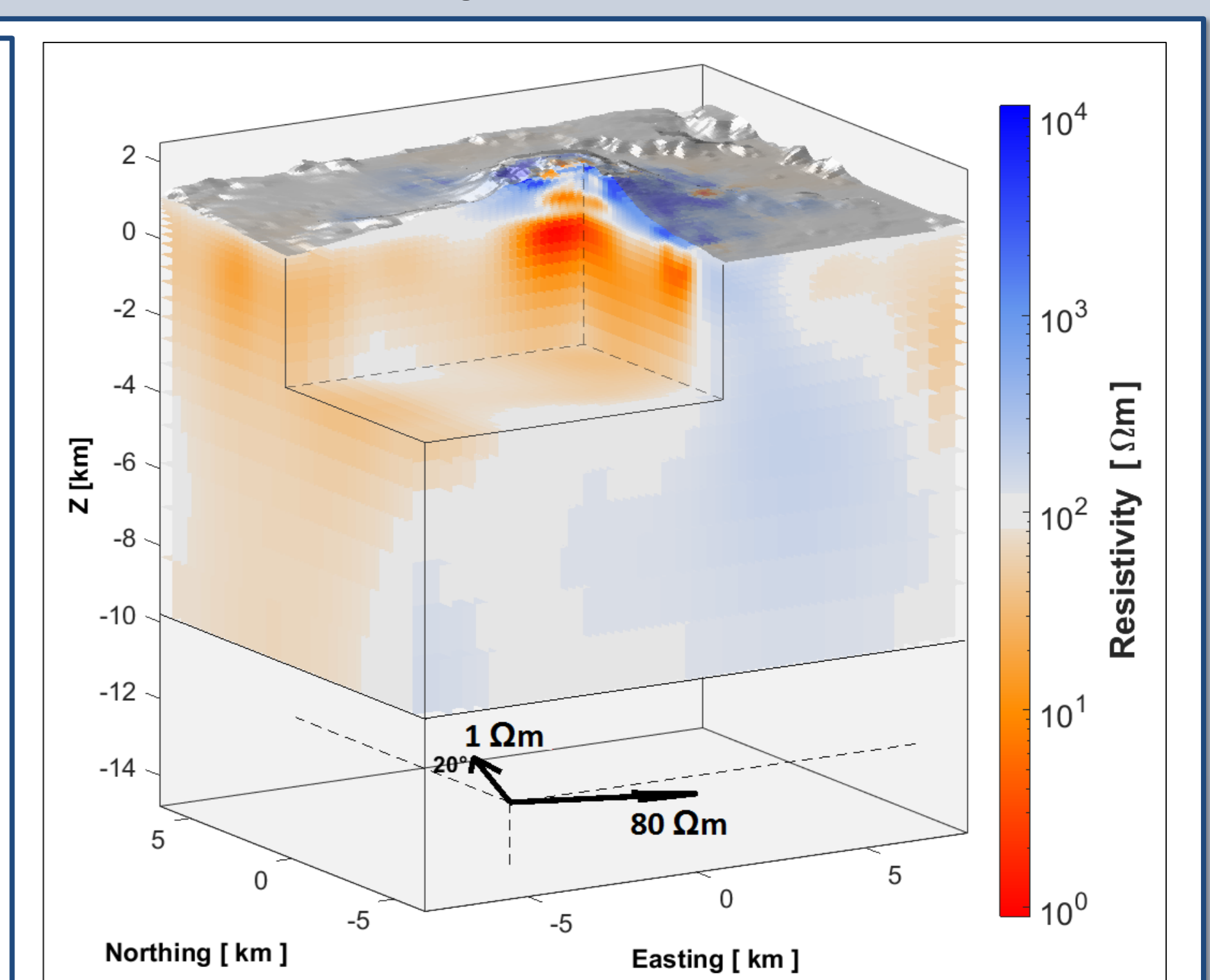


Fig. 5: An additional 3-D anisotropic forward model was calculated in Comsol multiphysics. The upper part of the model included the results from the isotropic inversion (without the large contrasts outside the measurement area). At 10 km depth, an anisotropic layer was added (30 km thick, resistivities 1 Ωm (North) and 80 Ωm (East), rotated by 20° (clockwise)). The model improves the data fit at the long periods (cf. **Fig. 6**). However, deviations in the Tipper Vector responses implicate room for improvements.

Conclusions: The RT and RPT tensors are useful tools to interpret complex MT data sets and allow for conclusions on resistivity structures prior to inversion or modeling approaches. The anisotropic forward model of the Ceboruco volcano provides a geologically reasonable alternative to the isotropic inversion results (conductive axis is parallel to the extension direction of the TZR → ductile deformation?).

References:

- Brown, C. (2016). Magnetotelluric tensors, electromagnetic field scattering and distortion in three-dimensional environments. *Journal of Geophysical Research: Solid Earth*, 121, 7040–7053. doi: 10.1002/2016JB013035
- Caldwell, T.G., Bibby, H.M., & Brown, C. (2004). The magnetotelluric phase tensor. *Geophys. J. Int.*, 158, 457–469.
- Egbert, G. (1997). Robust multiple-station magnetotelluric data processing. *Geophys. J. Int.* 130, S. 475–496.
- Hering, P., Brown, C., & Junge, A. (2019). Magnetotelluric Apparent Resistivity Tensors for improved Interpretations and 3-D Inversions. *J. Geophys. Res. Solid Earth*. Doi 10.1029/2018JB017221
- Hering, P. (2019). *Advances in Magnetotelluric Data Processing, Interpretation and 3-D Inversion, illustrated by a three-dimensional Resistivity Model of the Ceboruco Volcano*. Dissertation, Goethe-Universität Frankfurt.
- Kelbert, A., N. Meqbel, G. D. Egbert, & K. Tandon (2014). *Modem: A modular system for inversion of electromagnetic geophysical data*, *Computers & Geosciences*, 66, 40–53.